Journal of Membrane Science 360 (2010) 476–482

Contents lists available at ScienceDirect

Journal of Membrane Science

journal homepage: www.elsevier.com/locate/memsci

Highlighting pitfalls in the Maxwell–Stefan modeling of water–alcohol mixture permeation across pervaporation membranes

Rajamani Krishna*, Jasper M. van Baten

Van't Hoff Institute for Molecular Sciences, University of Amsterdam, Science Park 904, 1098 XH Amsterdam, The Netherlands

ARTICLE INFO

Article history:
Received 5 May 2010
Received in revised form 18 May 2010
Accepted 21 May 2010
Available online 1 June 2010

Keywords:
Zeolites
Molecular Dynamics
Membrane pervaporation
Water–alcohol mixtures
Adsorption
Maxwell–Stefan diffusion
Correlation effects
Hydrogen bonding

ABSTRACT

The Maxwell–Stefan (M–S) equations are widely used for modeling permeation of water–alcohol mixtures across microporous membranes in pervaporation and dehydration process applications.

For binary mixtures, for example, the following set of assumptions is commonly invoked, either explicitly or implicitly. (1) The M–S diffusivities $Đ_1$, and $Đ_2$, that portray interactions of individual components with the pore-walls, can be identified with the corresponding values for *pure* component permeation. (2) The $Đ_i$ are independent of the adsorbed phase mole fractions x_i of the permeating mixture within the pores. (3) The exchange coefficient, $Đ_{12}$, that signify correlations in diffusional jumps within the pores, can be estimated on the basis of the logarithmic interpolation formula $Đ_{12} = (Đ_{12}^{x_1 \to 1})^{x_1} (Đ_{12}^{x_2 \to 1})^{x_2}$, suggested by Vignes [Diffusion in binary solutions, Ind. Eng. Chem. Fund. 5 (1966) 189–199] for diffusion in binary liquid mixtures. (4) For structures such as LTA and DDR that consist of cages separated by narrow windows of sizes in the 0.35–0.42 nm range, the exchange coefficient is often assumed to have a large value, $Đ_{12} \to \infty$, leading to a set of un-coupled M–S equations.

Molecular Dynamics (MDs) simulations of diffusion in binary mixtures containing water, methanol, and ethanol in FAU, and LTA have been carried out to test each of the foregoing set of assumptions. The break-down of all four assumptions when applied to diffusion of water–alcohol mixture permeation is highlighted. The root-cause of this break-down can be traced to the hydrogen bonding between water and alcohol molecules, which is much more predominant than for water–water, and alcohol–alcohol molecule-pairs.

1. Introduction

Microporous zeolite membranes have been applied on an industrial scale for production of fuel grade ethanol by pervaporation [1]. For modeling permeation of water–alcohol mixtures across microporous membranes in pervaporation and dehydration applications, the fluxes N_i are commonly related to the chemical potential gradients $\nabla\mu_i$ by use of the Maxwell–Stefan (M–S) equations [2–21]:

$$-\phi \frac{c_i}{RT} \nabla \mu_i = \sum_{\substack{j=1 \\ j \neq i}}^{2} \frac{x_j N_i - x_i N_j}{Đ_{ij}} + \frac{N_i}{Đ_i}; \quad i = 1, 2 \tag{1}$$

where ϕ represents the fractional pore volume of the microporous crystalline material, and the concentrations c_i are defined in terms of accessible pore volume of the crystalline microporous layer. The fluxes N_i are defined in terms of the cross-sectional area of the crystalline framework. The x_i in Eq. (1) is the component mole fractions of the adsorbed phase within the microporous structures:

$$x_i = \frac{c_i}{c_t}; \quad i = 1, 2 \tag{2}$$

The $Đ_i$ characterize species i – wall interactions in the broadest sense. The $Đ_{12}$ are exchange coefficients representing interaction between components i with component j. At the molecular level, the $Đ_{ij}$ reflect how the facility for transport of species i *correlates* with that of species j. Conformity with the Onsager reciprocal relations prescribes

$$Đ_{12} = Đ_{21} \tag{3}$$

Formally speaking, the M–S equations (1) serve only to *define* the phenomenological coefficients $Đ_1$, $Đ_2$, and $Đ_{12}$. In practice, a number of assumptions and simplifications are commonly invoked in the application of Eq. (1) to the modeling of membrane permeation. These assumptions are listed below:

(1) The $Đ_1$ and $Đ_2$, can be identified with the corresponding M–S diffusivity for *unary* diffusion, evaluated at the same total load-

* Corresponding author. Tel.: +31 20 6270990; fax: +31 20 5255604.
E-mail address: r.krishna@uva.nl (R. Krishna).

0376-7388/$ – see front matter © 2010 Elsevier B.V. All rights reserved.
doi:10.1016/j.memsci.2010.05.049

ing or occupancy θ_t:

$$\theta_t = \sum_{i=1}^{2} \theta_i = \sum_{i=1}^{2} \frac{c_i}{c_{i,\text{sat}}} \tag{4}$$

where $c_{i,\text{sat}}$ is the saturation loading. This has the implication that the $Đ_i$ in the mixture should be independent of the partner species. Put another way, for water(1)–methanol(2) diffusion, the value of $Đ_1$ at any given mixture occupancy θ_t should be the same as for water(1)–ethanol(2) diffusion.

(2) While the dependence of $Đ_1$ and $Đ_2$ on the total loading $c_t = c_1 + c_2$, or occupancy θ_t, are commonly accounted for in modeling exercises [7,21], these coefficients are invariably assumed to be independent of the adsorbed phase composition, x_i.

(3) The exchange coefficient $Đ_{12}$ are not easily accessible from experiments. It is most commonly modeled using an interpolation formula that is based on the Vignes [22] model for diffusion in liquid mixtures:

$$Đ_{12} = (Đ_{12}^{x_1 \to 1})^{x_1} (Đ_{12}^{x_2 \to 1})^{x_2} = (Đ_{11})^{x_1} (Đ_{22})^{x_2} \tag{5}$$

For diffusion within microporous materials, the $Đ_{ii}$ are the self-exchange coefficients, that are determinable from MD simulations of unary diffusion of both $Đ_i$, and the self-diffusivity, $D_{i,\text{self}}$, by use of the following relationship:

$$\frac{1}{D_{i,\text{self}}} = \frac{1}{Đ_i} + \frac{1}{Đ_{ii}} \tag{6}$$

The ratio $Đ_i/Đ_{ii}$ can be viewed as a measure of the degree of correlations for unary diffusion of species i. As illustration, Fig. 1a presents MD data for CH_4, water, methanol, and ethanol diffusion in FAU at 300 K. The degree of correlations increases with loading, c_i. This is because the number of vacant sites within the structure decreases with increasing loading. Consequently, the number of times a molecule has to return to recently vacated sites increases with c_i; this accounts for increasing correlations. The degree of correlations also depends on the pore size, connectivity and topology. Fig. 1b presents a comparison of $Đ_i/Đ_{ii}$ data for CH_4 diffusion in FAU, MFI, and LTA. The intersecting channel structures of MFI experience the highest degree of correlations. Since experimental data on the exchange coefficients are rarely available, it is quite common in the literature to invoke the assumption that $Đ_i/Đ_{ii} \approx 1$, because of the lack of adequate information on the degree of correlations.

(4) In some special cases a further simplification is invoked with respect to the exchange coefficient $Đ_{12}$, when modeling permeation across LTA and DDR membranes [5,7]. For such zeolites, correlation effects are commonly assumed to be of negligible importance the windows separating the cages are in the 0.35–0.42 nm size range, allowing only one molecule at a time to hop from one cage to the neighboring one.

$$\frac{Đ_i}{Đ_{ii}} \to 0; \quad \frac{Đ_i}{Đ_{12}} \to 0; \quad i = 1, 2 \,(\text{negligible correlations}) \tag{7}$$

From the data presented in Fig. 1b it can be noted that Eq. (7) is perhaps a reasonable approximation for loadings $c_i < 10\,\text{kmol m}^{-3}$. When correlations are of negligible importance the contribution of the first right member of Eq. (1) can be ignored with respect to the second right member, leading to a set of un-coupled equations:

$$N_i = -\phi \frac{c_i}{RT} Đ_i \nabla \mu_i; \quad i = 1, 2 \,(\text{negligible correlations}) \tag{8}$$

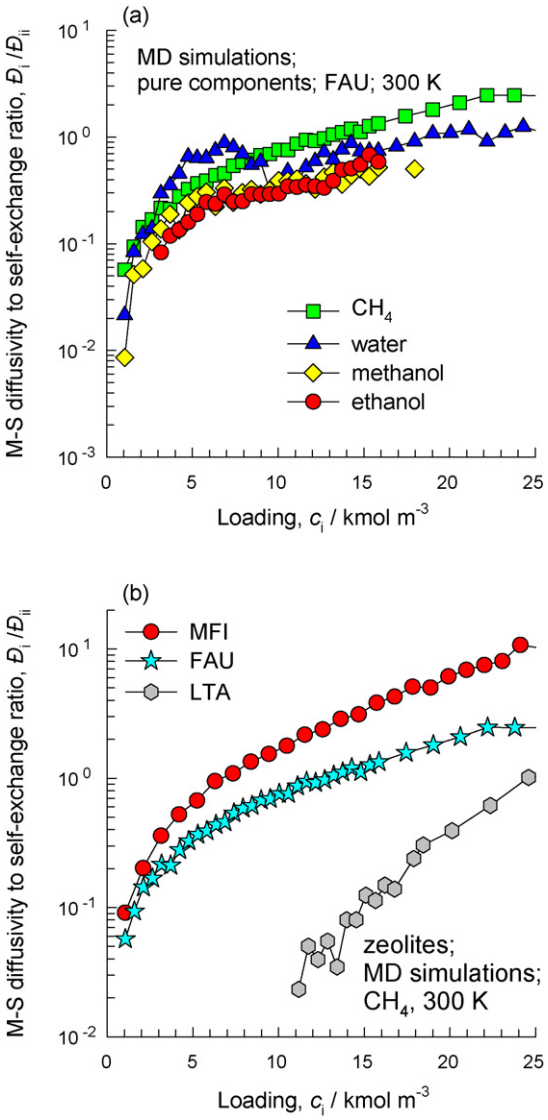

Fig. 1. (a) Ratio of the M–S diffusivity $Đ_i$ with respect to self-exchange coefficient $Đ_{ii}$ for CH_4, water, methanol, and ethanol diffusion in FAU at 300 K. (b) Comparison of MD data on $Đ_i/Đ_{ii}$ for CH_4 diffusion in FAU, MFI, and LTA.

Furthermore, the assumption of negligible correlations also implies that

$$D_{i,self} \approx Đ_i; \quad (\text{negligible correlations}) \tag{9}$$

for both unary and mixture diffusion.

The main objective of this work is to highlight the break-down of all four of the afore-mentioned assumptions when describing permeation of water–alcohol mixtures across microporous membranes. To achieve these objectives Molecular Dynamics (MDs) simulations of diffusion of water–methanol, water–ethanol, and methanol–ethanol, mixtures in FAU, and LTA zeolites were carried out. Diffusion in fluid mixtures, without the restraining influence of pore-walls, was also investigated in order to obtain a clear scientific picture of the underlying physico-chemical principles. The current work is an extension, and amplification, of previous publications [23–25] in which the significant influence of molecular clustering on diffusion characteristics in microporous materials have been underlined. A small portion of earlier MD simulation results [25], have been included in the present work in order to provide a comprehensive palette of data and concepts that will be

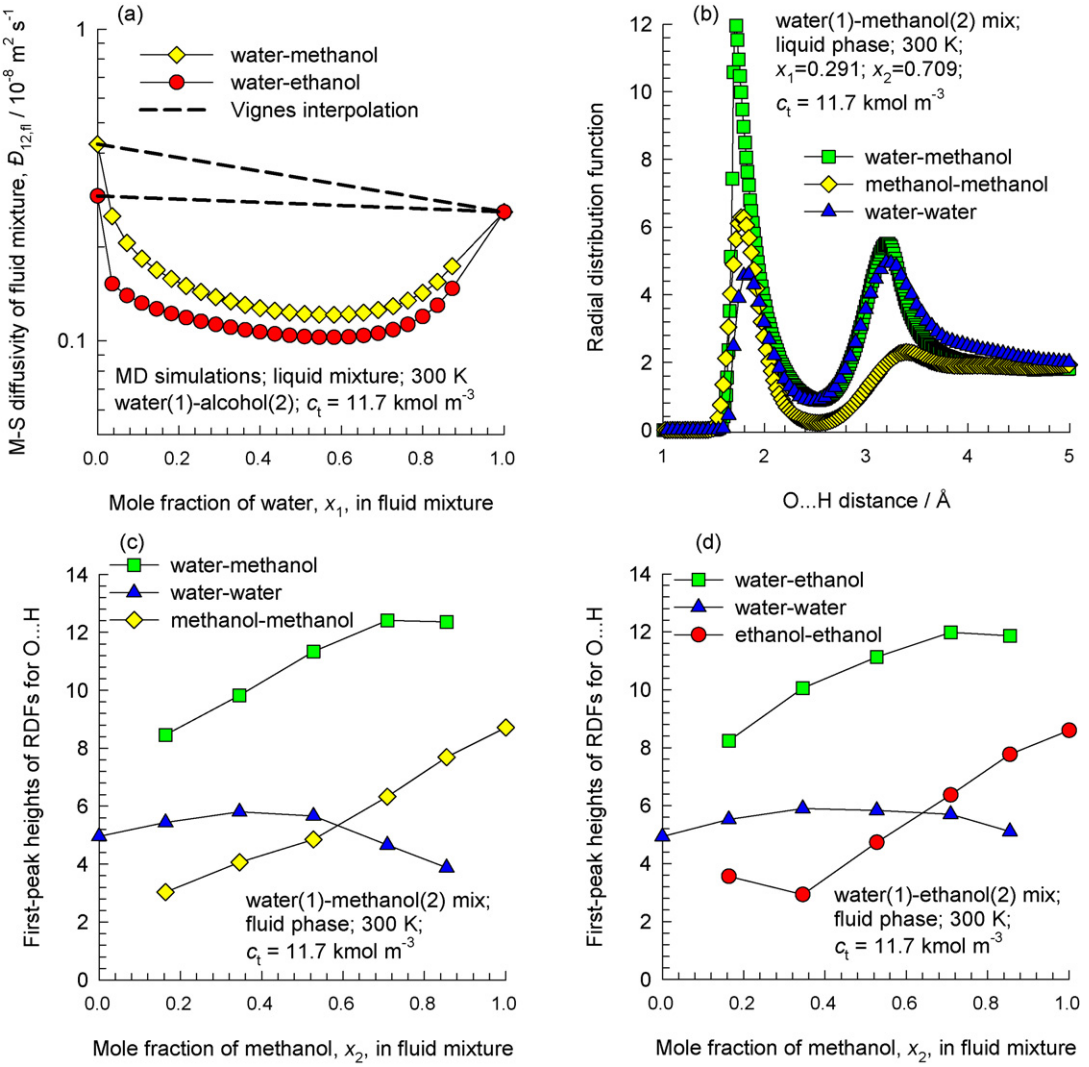

Fig. 2. (a) MD simulations of Maxwell–Stefan (M–S) diffusivities, $Đ_{12}$, for water–methanol and water–ethanol mixtures in a fluid mixture at a total concentration c_t = 11.7 kmol m^{-3}. The dashed lines represent calculations using the Vignes interpolation formula (5). (b) RDFs for binary liquid mixture of water and methanol at 300 K at a total concentration c_t = 11.7 kmol m^{-3}. (c) Plots of the first-peak heights of the RDFs, from data such as those presented in (b), for water(1)–methanol(2) liquid mixtures at 300 K. (d) Plots of the first-peak heights of the RDFs, from for water(1)–ethanol(2) liquid mixtures at 300 K.

useful to a practicing membrane technologist for modeling purposes.

The simulation methodologies, along with details of the force fields used are exactly as that described in our earlier publication [25]; this information is not repeated here.

2. The Vignes interpolation formula

Let us begin by examining the validity of the Vignes interpolation formula (5) for water(1)–methanol(2), and water(1)–ethanol(2) mixtures in the *liquid* phase. MD simulations for the two binary mixtures are shown in Fig. 2a. The Vignes formula is seen to severely overpredict the variation of $Đ_{12}$ with x_1 for both liquid mixtures. Available experimental data confirm the trend portrayed in the MD simulations [26–28]. The failure of the Vignes interpolation is traceable to strong hydrogen bonding between water and alcohol molecular pairs. This is evidenced in the data on radial distribution functions (RDFs) presented in Fig. 2b for O–H bond distances for water–water, water–methanol, and methanol–methanol pairs in water–methanol mixtures. The first peaks occur at distances smaller than 2 Å, that is characteristic of hydrogen bonding [29]. Collecting information on the first-peak heights for water–methanol mixtures for a variety of compositions, Fig. 2c can be constructed. The first-peak heights for water–methanol pairs are significantly higher than for water–water and methanol–methanol, indicating the much stronger bonding between water and methanol. A similar situation manifests for water–ethanol mixtures; see Fig. 2d. The significantly stronger hydrogen bonding between water–alcohol molecular pairs causes the significant deviation from Vignes estimations.

Fig. 3a presents a plot of the first-peak heights of the RDFs for methanol(1)–ethanol(2) liquid mixtures at 300 K. It is observed that the first-peak heights for each of the molecule-pairs are nearly the same and there are no significant differences in the degrees of hydrogen bonding. As a logical consequence, the Vignes interpolation formula should be expected to hold for methanol–ethanol mixtures. This is indeed found to be the case, as evidenced by the MD simulation results for $Đ_{12}$ presented in Fig. 2b. The data of Figs. 2 and 3 imply that it is not hydrogen bonding, *per se*, that contributes to deviation from the Vignes formula; rather, it is the *difference* in the degrees of hydrogen bonding between constituent molecular pairs.

The failure of the Vignes interpolation formula for water–alcohol liquid mixtures bodes a corresponding failure

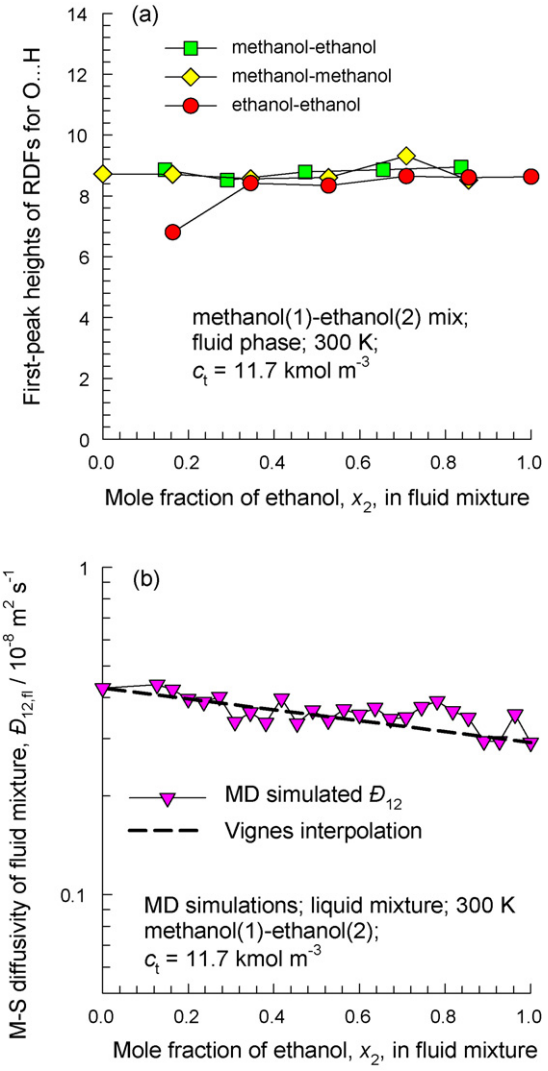

Fig. 3. (a) Plots of the first-peak heights of the RDFs for methanol(1)–ethanol(2) liquid mixtures at 300 K. (b) MD simulations of Maxwell–Stefan (M–S) diffusivities, $Đ_{12}$, for methanol(1)–ethanol (2) mixtures in a fluid mixture at a total concentration c_t = 11.7 kmol m^{-3}.

for diffusion within microporous structures. This is confirmed by MD simulations of $Đ_{12}$ for water–methanol and water–ethanol mixtures in FAU zeolite; see Fig. 4a. The reasons for this failure are also to be attributable to stronger hydrogen bonding between water–alcohol pairs than water–water and alcohol–alcohol pairs in the adsorbed phase within the pores of FAU. By the same token, we should expect the $Đ_{12}$ for methanol–ethanol diffusion in FAU to obey the Vignes prescription and this is indeed found to be the case; see Fig. 4b.

The success of the Vignes formula for methanol–ethanol diffusion is symptomatic for mixtures of non-polar molecules in microporous materials. To confirm this we present data for diffusion on C_3H_8–nC_4H_{10} in FAU in Fig. 4c. Put another way, the Vignes interpolation has good estimation capabilities for mixtures of non-polar, and for mixture in which the differences in the hydrogen bonding between molecular pairs are small.

3. Is $Đ_i$ in the mixture same as for pure component?

Fig. 5 presents data on MD simulated values of M–S diffusivities, $Đ_i$, of (a) water, (b) methanol, and (c) ethanol in equimolar ($c_1 = c_2$) water–methanol, water–ethanol and methanol–ethanol mixtures

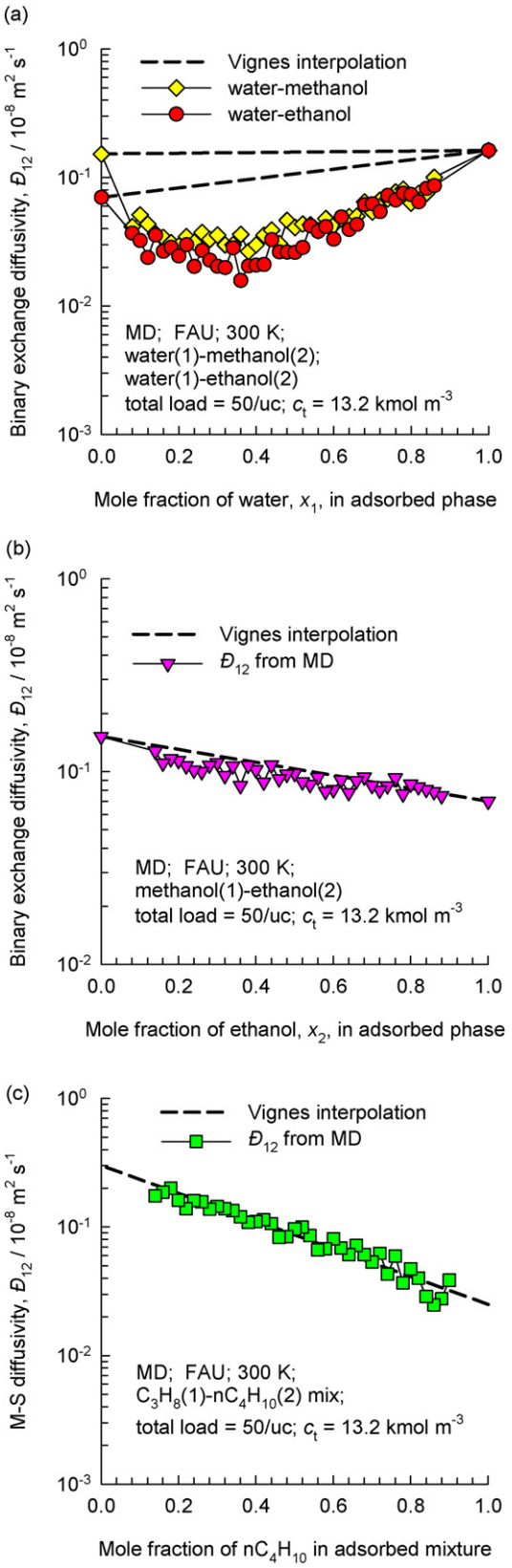

Fig. 4. MD simulations of binary exchange coefficients, $Đ_{12}$, for diffusion of (a) water–methanol, water–ethanol mixtures, (b) methanol–ethanol, and (c) C_3H_8–nC_4H_{10} mixtures in FAU at 300 K. The total loading in the mixture is held constant at 50 molecules per unit cell, corresponding to a total concentration c_t = 13.2 kmol m^{-3}.

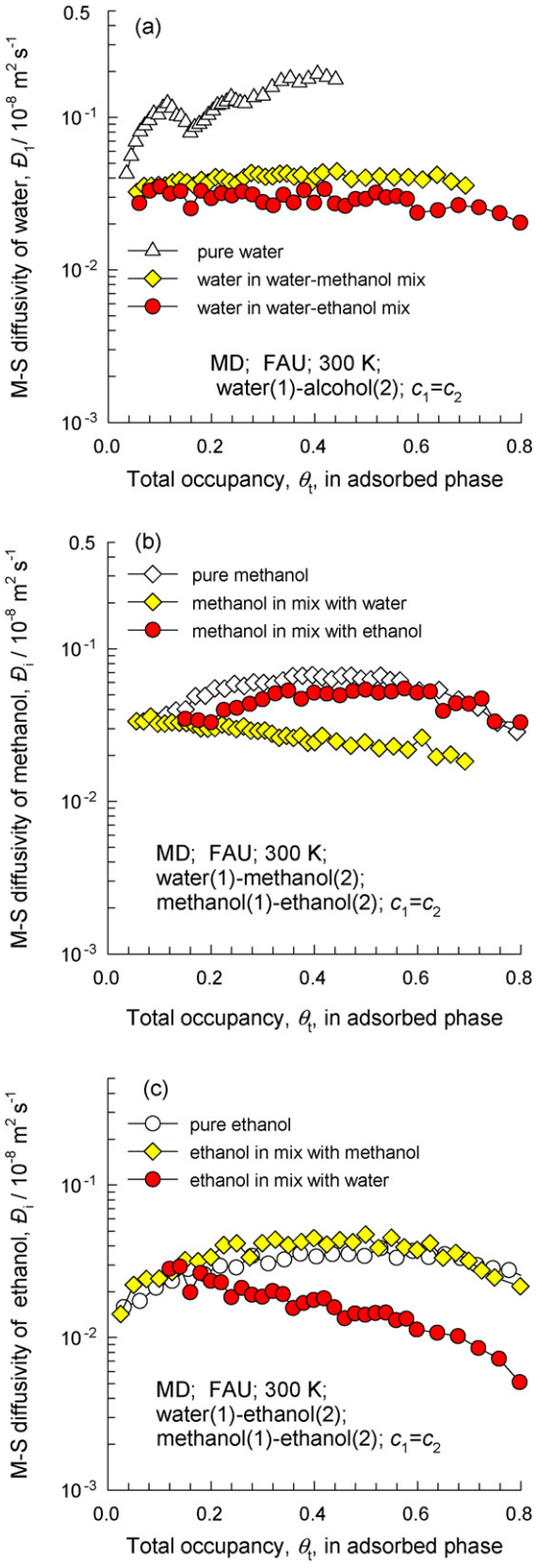

Fig. 5. MD simulated values of M–S diffusivities, $Đ_i$, of (a) water, (b) methanol, and (c) ethanol in equimolar ($c_1 = c_2$) water–methanol, water–ethanol and methanol–ethanol mixtures in FAU at 300 K. Also shown are the pure component $Đ_i$ determined at the same total mixture occupancy θ_t in water–methanol and water–ethanol mixtures. The total occupancy is determined using the saturation capacities $c_{i,sat} = 60$, 28, and 17 kmol m^{-3} for water, methanol and ethanol, respectively.

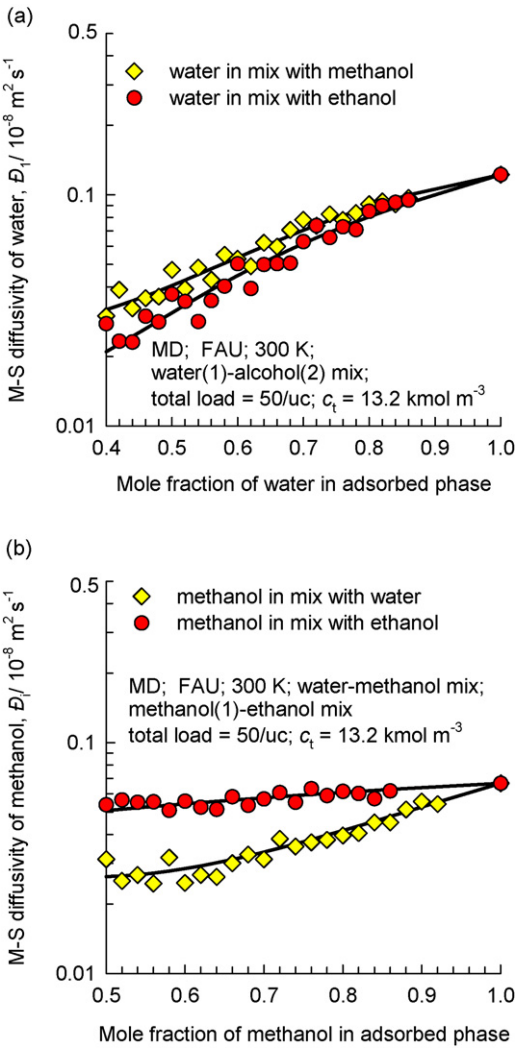

Fig. 6. (a) MD simulations of M–S diffusivities, $Đ_1$, of water in water–methanol and water–ethanol mixtures in FAU at 300 K. (b) MD simulations of M–S diffusivities, $Đ_i$, of methanol in water–methanol and methanol–ethanol mixtures in FAU at 300 K. In both (a) and (b), the total loading in the mixture is held constant at 50 molecules per unit cell, corresponding to a total concentration $c_t = 13.2$ kmol m^{-3}.

in FAU at 300 K. Also shown are the pure component $Đ_i$ determined at the same total mixture occupancy θ_t in water–methanol and water–ethanol mixtures.

From Fig. 5a it can be observed that the $Đ_i$ of water in mixtures with alcohols are significantly lower than that for pure water. The reason for this is that due to hydrogen bonding, water tends to cluster around alcohol molecules. The mobility of water molecules in the mixtures is significantly lowered due to cluster formation.

Interestingly, the $Đ_i$ of methanol in mixtures with water is also significantly lower than the value for pure methanol; see Fig. 5b. In sharp contrast, the $Đ_i$ of methanol in mixtures with ethanol is practically the same as for pure methanol. This result is consonant with the exchange coefficient data presented in Fig. 4b. The hydrogen bonding between methanol–ethanol and methanol–methanol is significantly weaker than for water–methanol pairs.

The results for the M–S diffusivity of ethanol are analogous to those for methanol; see Fig. 5c. Compared with pure ethanol, the $Đ_i$ is significantly lowered in mixtures with water, but in remains practically the same in mixtures with methanol.

The influence of mixture composition on the $Đ_i$ in mixtures will now be examined. Fig. 6a presents data for $Đ_1$ of water in binary mixtures with methanol and ethanol. For both mixtures, we note a

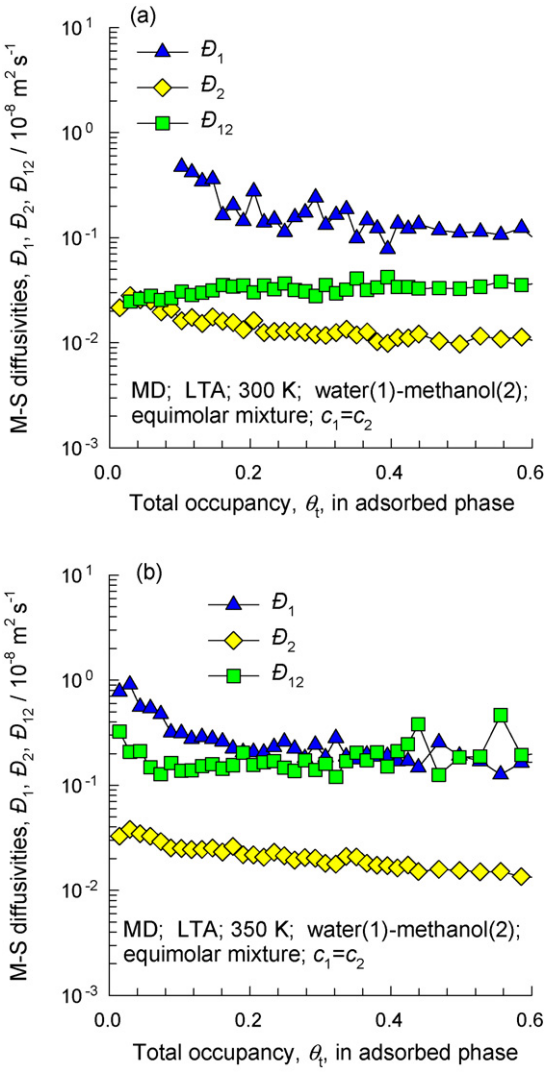

Fig. 7. MD simulated values of M–S diffusivities, $Đ_1$, $Đ_2$, and $Đ_{12}$ for diffusion of equimolar water(1)–methanol(2) mixtures in LTA at (a) 300 K and (b) 350 K. The total occupancy θ_t is determined using the saturation capacities $c_{i,sat} = 60$, and 28 kmol m^{-3} for water, and methanol, respectively.

reduction in the $Đ_1$ of water with increasing alcohols concentration within the pores. Furthermore, the mobility of water in mixtures with ethanol is slightly lower than for water–methanol mixtures. The data in Fig. 6a provide a fundamental rationale for experimental observations that the water permeance is significantly reduced by the presence of alcohol in a variety of microporous membranes [6,30,31].

Fig. 6b presents data for the M–S diffusivity $Đ_i$ of methanol in water–methanol and methanol–ethanol mixtures. For methanol–ethanol mixtures the M–S diffusivity $Đ_i$ is practically independent of composition, whereas in mixtures with water, the $Đ_i$ decreases significantly below the pure component value with increasing water concentrations. Water–methanol clustering is much more significant than methanol–ethanol clustering.

The results presented in Figs. 5 and 6 indicate that for a certain range of compositions of water–alcohol mixtures there is *mutual hindering of both components* in the mixture. For water–alcohols diffusion we need to take account not only of the dependence of $Đ_i$ with total pore concentration, c_t, but also, additionally the influence of the composition of the mixture.

There is some experimental evidence of such mutual hindering for permeation of acetone–methanol mixtures across an MFI membrane [32]. Yu et al. [32] found that their experimental data on permeation of methanol–acetone mixtures across an MFI membrane can only be rationalized if both the component $Đ_i$, are lowered in the mixture, when compared with the pure component values. The underlying cause of their findings is most likely to be due to the clustering caused by hydrogen bonding of acetone and methanol molecules, and evidence of such clustering is provided by molecular simulations [33].

4. Can we assume un-coupled diffusion for LTA and DDR?

For zeolites such as LTA and DDR the commonly made assumption in practice is that the correlation effects are of negligible importance [5,7], and for modeling purposes it is common to invoke Eq. (8). In order to test this assumption we carried out MD simulations to determine $Đ_1$, $Đ_2$, and $Đ_{12}$ for equimolar water(1)–methanol(2) mixtures in LTA for a variety of loadings at temperatures of 300 K and 350 K; see Fig. 7.

The simulations show that $Đ_{12}$ is intermediate in value between $Đ_1$ and $Đ_2$ and the assumptions required for negligible correlations, Eq. (7), do not hold over the entire range of occupancies θ_t.

In the study by Kuhn et al. [7] for water–alcohols pervaporation across a DDR membrane, it was found that the use of un-coupled Eq. (8), with the $Đ_1$ and $Đ_2$ determined from unary permeation data, lead to a severe overestimation of the permeation fluxes. On the basis of the results presented here, we can trace this poor agreement to a combination of two factors: (1) the $Đ_i$ in the mixture is lower than that of the pure components, and (2) correlation effects cannot be considered to be negligible.

5. Conclusions

For water–alcohol mixtures, the hydrogen bonding between water and alcohol molecules is much stronger than for water–water, and alcohol–alcohol pairs. This leads to a break-down of some commonly made assumptions in the Maxwell–Stefan modeling of membrane permeation.

(1) The Maxwell–Stefan diffusivity, $Đ_i$, of either component in water–alcohol mixtures are lower than the corresponding values of the pure components. In practice we need to take account of the influence of mixture composition on the $Đ_i$ and on the partner species.
(2) The Vignes interpolation formula (5) fails to account for the variation of $Đ_{12}$ with composition. Correlation effects are significantly stronger in water–alcohol mixtures than for the constituent species.
(3) For zeolites such as LTA and DDR the assumption of un-coupled equations (8) is not justified for water–alcohols permeation.

Acknowledgements

RK acknowledges the grant of a TOP subsidy from the Netherlands Foundation for Fundamental Research (NWO-CW) for intensification of reactors.

Nomenclature

Notation

c_i	concentration of species i, mol m^{-3}
$c_{i,sat}$	saturation capacity of species i, mol m^{-3}
c_t	total concentration in mixture, mol m^{-3}

$Đ_i$	M–S diffusivity defined by Eq. (1), $m^2\ s^{-1}$
$Đ_{ii}$	M–S self-exchange coefficient, $m^2\ s^{-1}$
$D_{i,self}$	self-diffusivity of species i, $m^2\ s^{-1}$
$Đ_{12}$	Binary exchange coefficient defined by Eq. (1), $m^2\ s^{-1}$
$Đ_{12,fl}$	M–S binary diffusivity for fluid mixture, $m^2\ s^{-1}$
N_i	molar flux of species i, based on crystalline framework area, $mol\ m^{-2}\ s^{-1}$
R	gas constant, $8.314\ J\ mol^{-1}\ K^{-1}$
t	time, s
T	absolute temperature, K
x_i	mole fraction of species i based on loading within pore

Greek letters

ϕ	fractional pore volume of zeolite
μ_i	molar chemical potential, $J\ mol^{-1}$
θ_i	fractional occupancy of species i
θ_t	total occupancy of mixture

Subscripts

i	referring to component i
fl	referring to fluid phase
sat	referring to saturation conditions
t	referring to total mixture

Vector and matrix notation

∇	gradient operator

References

[1] K. Sato, K. Aoki, K. Sugimoto, K. Izumi, S. Inoue, J. Saito, S. Ikeda, T. Nakane, Dehydrating performance of commercial LTA zeolite membranes and application to fuel grade bio-ethanol production by hybrid distillation/vapor permeation process, Microporous Mesoporous Mater. 115 (2008) 184–188.

[2] J. Caro, M. Noack, Zeolite membranes—recent developments and progress, Microporous Mesoporous Mater. 115 (2008) 215–233.

[3] S.L. Wee, C.T. Tye, S. Bhatia, Membrane separation process—pervaporation through zeolite membrane, Sep. Purif. Technol. 63 (2008) 500–516.

[4] T.C. Bowen, R.D. Noble, J.L. Falconer, Fundamentals and applications of pervaporation through zeolite membranes, J. Membr. Sci. 245 (2004) 1–33.

[5] M. Pera-Titus, C. Fité, V. Sebastián, E. Lorente, J. Llorens, F. Cunill, Modeling pervaporation of ethanol/water mixtures within 'real' zeolite NaA membranes, Ind. Eng. Chem. Res. 47 (2008) 3213–3224.

[6] J. Kuhn, K. Yajima, T. Tomita, J. Gross, F. Kapteijn, Dehydration performance of a hydrophobic DD3R zeolite membrane, J. Membr. Sci. 321 (2008) 344–349.

[7] J. Kuhn, J.M. Castillo-Sanchez, J. Gascon, S. Calero, D. Dubbeldam, T.J.H. Vlugt, F. Kapteijn, J. Gross, Adsorption and diffusion of water, methanol, and ethanol in all-silica DD3R: experiments and simulation, J. Phys. Chem. C 113 (2009) 14290–14301.

[8] B. Tokay, J.L. Falconer, R.D. Noble, Alcohol and water adsorption and capillary condensation in MFI zeolite membranes, J. Membr. Sci. 334 (2009) 23–39.

[9] F. Kapteijn, J.A. Moulijn, R. Krishna, The generalized Maxwell–Stefan model for diffusion in zeolites: sorbate molecules with different saturation loadings, Chem. Eng. Sci. 55 (2000) 2923–2930.

[10] A.I. Skoulidas, D.S. Sholl, R. Krishna, Correlation effects in diffusion of CH_4/CF_4 mixtures in MFI zeolite. A study linking MD simulations with the Maxwell–Stefan formulation, Langmuir 19 (2003) 7977–7988.

[11] S. Chempath, R. Krishna, R.Q. Snurr, Nonequilibrium MD simulations of diffusion of binary mixtures containing short n-alkanes in faujasite, J. Phys. Chem. B 108 (2004) 13481–13491.

[12] R. Krishna, J.M. van Baten, Diffusion of alkane mixtures in zeolites. Validating the Maxwell–Stefan formulation using MD simulations, J. Phys. Chem. B 109 (2005) 6386–6396.

[13] R. Krishna, J.M. van Baten, The Darken relation for multicomponent diffusion in liquid mixtures of linear alkanes. An investigation using Molecular Dynamics (MD) simulations, Ind. Eng. Chem. Res. 44 (2005) 6939–6947.

[14] R. Krishna, J.M. van Baten, Describing binary mixture diffusion in carbon nanotubes with the Maxwell–Stefan equations. An investigation using molecular dynamics simulations, Ind. Eng. Chem. Res. 45 (2006) 2084–2093.

[15] R. Krishna, J.M. van Baten, Insights into diffusion of gases in zeolites gained from molecular dynamics simulations, Microporous Mesoporous Mater. 109 (2008) 91–108.

[16] R. Krishna, J.M. van Baten, Onsager coefficients for binary mixture diffusion in nanopores, Chem. Eng. Sci. 63 (2008) 3120–3140.

[17] R. Krishna, J.M. van Baten, Unified Maxwell–Stefan description of binary mixture diffusion in micro- and mesoporous materials, Chem. Eng. Sci. 64 (2009) 3159–3178.

[18] R. Krishna, Describing the diffusion of guest molecules inside porous structures, J. Phys. Chem. C 113 (2009) 19756–19781.

[19] J. Kuhn, R. Stemmer, F. Kapteijn, S. Kjelstrup, J. Gross, A non-equilibrium thermodynamics approach to model mass and heat transport for water pervaporation through a zeolite membrane, J. Membr. Sci. 330 (2009) 388–398.

[20] F. de Bruijn, J. Gross, Z. Olujić, P. Jansens, F. Kapteijn, On the driving force of methanol pervaporation through a microporous methylated silica membrane, Ind. Eng. Chem. Res. 46 (2007) 4091–4099.

[21] B. Bettens, A. Verhoef, H.M. van Veen, C. Vandecasteele, J. Degrève, B. van der Bruggen, Pervaporation of binary water–alcohol and methanol–alcohol mixtures through microporous methylated silica membranes: Maxwell–Stefan modeling, Comput. Chem. Eng. (2010), http://dx.doi.org/doi:10.1016/j.compchemeng.2010.03.014.

[22] A. Vignes, Diffusion in binary solutions, Ind. Eng. Chem. Fund. 5 (1966) 189–199.

[23] R. Krishna, J.M. van Baten, Investigating cluster formation in adsorption of CO_2, CH_4, and Ar in zeolites and metal organic frameworks at sub-critical temperatures, Langmuir 26 (2010) 3981–3992.

[24] R. Krishna, J.M. van Baten, Highlighting a variety of unusual characteristics of adsorption and diffusion in microporous materials induced by clustering of guest molecules, Langmuir 26 (2010) 8450–8463.

[25] R. Krishna, J.M. van Baten, Hydrogen bonding effects in adsorption of water–alcohol mixtures in zeolites and the consequences for the characteristics of the Maxwell–Stefan diffusivities, Langmuir (2010), http://dx.doi.org/10.1021/la100737c.

[26] Z.J. Derlacki, A.J. Easteal, A.V.J. Edge, L.A. Woolf, Z. Roksandic, Diffusion coefficients of methanol and water and the mutual diffusion coefficient in methanol–water solutions at 278 and 298 K, J. Phys. Chem. 89 (1995) 5318–5322.

[27] Y.E. Lee, S.F.Y. Li, Binary diffusion coefficients of the methanol/water system in the temperature range 30–40 °C, J. Chem. Eng. Data 36 (1991) 240–243.

[28] J.T. Su, P. Brent Duncan, A. Momaya, A. Jutila, D. Needham, The effect of hydrogen bonding on the diffusion of water in n-alkanes and n-alcohols measured with a novel single microdroplet method, J. Chem. Phys. 132 (2010) 044506.

[29] C. Zhang, X. Yang, Molecular dynamics simulation of ethanol/water mixtures for structure and diffusion properties, Fluid Phase Equilib. 231 (2005) 1–10.

[30] M. Nomura, T. Yamaguchi, S. Nakao, Ethanol/water transport through silicalite membranes, J. Membr. Sci. 144 (1998) 161–171.

[31] S. Khajavi, J.C. Jansen, F. Kapteijn, Application of hydroxy sodalite films as novel water selective membranes, J. Membr. Sci. 326 (2009) 153–160.

[32] M. Yu, J.L. Falconer, R.D. Noble, R. Krishna, Modeling transient permeation of polar organic mixtures through a MFI zeolite membrane using the Maxwell–Stefan equations, J. Membr. Sci. 293 (2007) 167–173.

[33] Y. Jia, X. Guo, Monte Carlo simulation of methanol diffusion in critical media, Chin. J. Chem. Eng. 14 (2006) 413–418.